Current Research in Pharmacology and Drug Discovery 2 (2021) 100059

Contents lists available at ScienceDirect

Current Research in Pharmacology and Drug Discovery

journal homepage: www.journals.elsevier.com/current-research-in-pharmacology-and-drug-discovery

# Interaction of obtusilactone B and related butanolide lactones with the barrier-to-autointegration factor 1 (BAF1). A computational study

Christian Bailly [a,*], Gérard Vergoten [b]

[a] OncoWitan, Lille, (Wasquehal), 59290, France
[b] University of Lille, Inserm, INFINITE - U1286, Institut de Chimie Pharmaceutique Albert Lespagnol (ICPAL), Faculté de Pharmacie, 3 rue du Professeur Laguesse, BP-83, F-59006, Lille, France

ARTICLE INFO

*Keywords:*
Barrier-to-autointegration factor 1
Butanolide lactones
Obtusilactone
Cancer

ABSTRACT

The barrier-to-autointegration factor 1 (BAF1) protein is a DNA-binding protein implicated in nuclear envelop repair and reformation after mitosis. This nuclear protein is frequently overexpressed in cancer cells and plays a role in the occurrence and development of different tumors. It is a potential therapeutic target for gastric cancer, breast cancer and other malignancies. For this reason, BAF1 inhibitors are searched. The butanolide lactone obtusilactone B (Ob-B) has been found to inhibit VRK1-dependent phosphorylation of BAF1, upon direct binding to the nuclear protein. Taking advantage of the known crystallographic structure of BAF1, we have elaborated molecular models of Ob-B bound to BAF1 to delimit the binding site and binding configuration. The long endoolefinic alkyl side chain of Ob-B extends into a small groove on the protein surface, and the adjacent exo-methylene-γ-lactone moiety occupies a pocket comprising to the Ser-4 phosphorylation site of BAF1. Twenty butanolide lactones structurally close to ObB were screened for BAF1 binding. Several natural products with BAF1-binding capacity potentially superior to Ob-B were identified, including mahubanolide, kotomolide B, epilitsenolide D2, and a few other known anticancer plant natural products. Our study provides new ideas to guide the discovery and design of BAF1 inhibitors.

## 1. Introduction

Despite major advances in recent years with the advent of novel immunotherapies, cancer remains a devastating disease worldwide. Novel approaches and targets are needed to combat cancers, in particular to treat advanced forms of cancers and associated metastatic diseases. Among new targets, those implicated in the organization and protection of genomic DNA are being increasingly considered (Gorjánácz, 2014). In this category, the Barrier-to-Autointegration Factor 1 (BAF1) is a target of choice as an essential protein for nuclear rupture repair. BAF1 is a DNA-binding protein involved in nuclear envelope reformation after mitosis (Halfmann and Roux, 2021) and plays a major role in the repair of DNA double-strand breaks through the regulation of DNA-dependent kinase (DNA-PK) activity (Burgess et al., 2021). It contributes to multiple aspects of genome maintenance (Wiebe and Jamin, 2016).

*Through DNA-binding,* BAF1 tethers chromatin to the nuclear envelope. *It also interacts with* LAP2-emerin-MAN1 (LEM)-domain proteins generally localized at the inner nuclear membrane. Phosphorylation of BAF1 by the protein kinase *vaccinia-related kinase 1 (VRK1)* regulates its DNA binding activity, its subcellular localization and dimerization (Nichols et al., 2006; Gorjánácz et al., 2007; Jamin et al., 2014). Both BAF1 and VRK1 are considered as valid targets for different cancer types, such as esophageal squamous cell carcinoma (Ren et al., 2020). BAF1 plays a role in the development of triple-negative breast cancer (Zhang, 2020), gastric cancer (Li et al., 2018), hepatocellular carcinoma (Shen et al., 2018) and other malignancies (Li et al., 2017).

Molecules directed against BAF1 or VRK1 are actively searched as anticancer agents. For examples, DNA aptamers targeting specifically VRK1 were found to efficiently block proliferation of MCF7 breast cancer cells (Carrión-Marchante et al., 2021). Various small molecules selectively targeting VRK1 have also been identified and designed (Couñago et al., 2017; Serafim et al., 2019). The flavonoid luteolin was found also to regulate cell cycle progression by modulating VRK1 activity, leading to the suppression of cancer cell proliferation and the induction of apoptosis (Kim et al., 2014). In contrast, there are very few compounds directly targeting BAF1. High throughput screening assays have been developed

*Abbreviations:* BAF1, Barrier-to-Autointegration Factor 1; Ob-B, obtusilactone B; VRK1, vaccinia-related kinase 1.

* Corresponding author.
*E-mail address:* christian.bailly@oncowitan.com (C. Bailly).

https://doi.org/10.1016/j.crphar.2021.100059
Received 16 August 2021; Received in revised form 8 September 2021; Accepted 20 September 2021

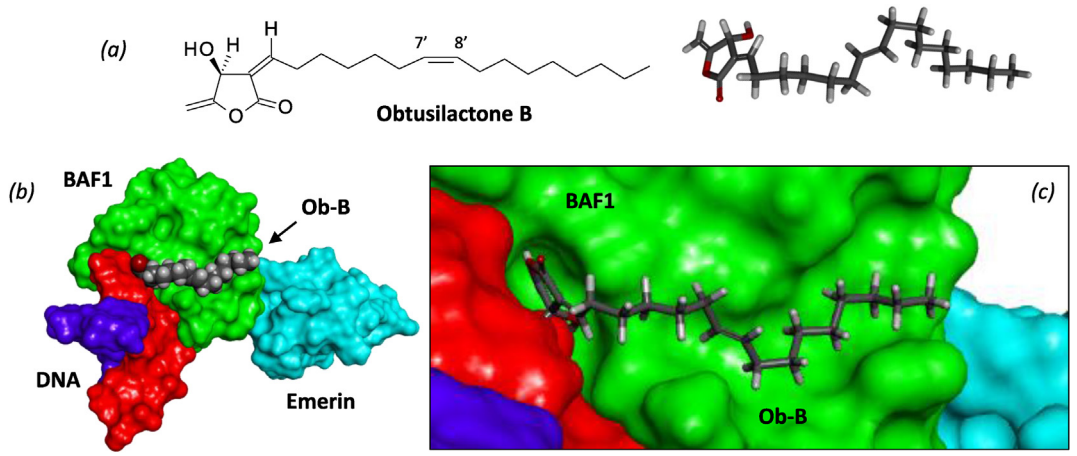


**Fig. 1.** (a) Structure of obtusilactone B (Ob-B). (b) A model of the compound bound to the ternary complex formed between BAF1 (in green), emerin (in cyan) and DNA (blue and red strands). (c) A close-up view of Ob-B lying in a groove at the surface of BAF1, lying from the DNA side to the emerin side. (For interpretation of the references to color in this figure legend, the reader is referred to the Web version of this article.)

to discover small molecule inhibitors of BAF-dependent DNA retention and to identify BAF1 inhibitors (Burger et al., 2020). The tetracyclic red dye brazilin, an anticancer compound isolated from the plant *Caesalpinia sappan*, has been shown to bind directly to BAF1 and to inhibit VRK1-mediated BAF1 phosphorylation (Kim et al., 2015). But the most interesting natural product BAF1 inhibitor is arguably the anticancer butanolide obtusilactone B (Ob-B, Fig. 1) isolated from a *n*-hexane extract of the stem of the plant *Machilus thunbergii* (Kim et al., 2013).

The name obtusilactone comes from the plant *Lindera* obtusiloba Blume (Dankbbai in Japanese), *from which the first* obtusilactone was isolated (Niwa et al., 1975a) together with the related compounds isoobtusilactone, obtusilactone A and isoobtusilactone A, all bearing an α-methylene-γ-butyrolactone ring (Niwa et al., 1975b). *L.* obtusiloba Blume contains compounds with a C17 or a C21 chain and some dimers (Niwa et al., 1977). Obtusilactone B and isoobtusilactone B are C21 derivatives both isolated form *L.* obtusiloba (Niwa et al., 1975c). Obtusilactone B was later isolated from *Machilus thunbergii* Siebold & Zucc. (known as Makko tree), a plant rich in butanolides and lignans (Bailly, 2021). Ob-B was found to target BAF1 and to suppress BAF1 phosphorylation by VRK1, so as to inhibit the disruption of the link between DNA and the nuclear envelop. This drug action blocks cell cycle progression of cancer cells and induces tumor cell death (Kim et al., 2013). A direct interaction between obtusilactone B and the purified BAF1 protein has been evidenced and an affinity constant ($K_D$) of 1.39 μM was calculated. A molecular modeling analysis has suggested that the heterocyclic moiety of the natural product is important for the interaction with the protein, in a glycine-rich groove (Kim et al., 2013). Ob-B could be considered as an archetype for the design of BAF1-regulatory agents.

Obtusilactones display marked anticancer properties. Ob-A is an inhibitor of the human mitochondrial Lon protease, which is frequently upregulated in non-small-cell lung cancer (NSCLC) cell lines. The compound down-regulates expression of the Lon protein, and triggers caspase-mediated apoptosis (Wang et al., 2010). The compound also displays osteogenic effects. It can stimulate new bone formation by bone marrow-derived mesenchymal stem cells (Lin et al., 2017). In the present study, we have investigated the binding of Ob-B to BAF1 using molecular modeling. Different crystallographic and NMR structures of BAF1 have been solved, for the free protein, and the protein bound to LEM-domain of emerin and to DNA (Umland et al., 2000; Bradley et al., 2005; Cai et al., 2007). Here we have used the X-ray structure of recombinant human BAF1 (PDB: 1CI4) to study the interaction of Ob-B with the protein. In addition, we investigated the interaction of twenty structurally related butanolide derivatives with the protein, in order to identify other potential BAF1 inhibitors.

**Table 1**
Calculated potential energy of interaction (ΔE) and free energy of hydration (ΔG) for the interaction of the indicated natural products with BAF1.

| Compounds | ΔE (kcal/mol) | ΔG (kcal/mol) |
|---|---|---|
| Obtusilatone B | −38.50 | −20.25 |
| Brazilin | −41.55 | −17.20 |
| Mahubanolide | −48.45 | −14.70 |
| Kotomolide B | −46.90 | −21.60 |
| Isomahubynolide | −46.55 | −21.40 |
| Isomahubanolide | −46.40 | −18.50 |
| Epilitsenolide D2 | −45.50 | −18.50 |
| Obtusilactone A | −45.30 | −18.70 |
| Litsealactone B | −44.50 | −16.00 |
| Isomahubenolide | −44.20 | −18.85 |
| Mahubynolide | −42.25 | −11.30 |
| Litsealactone A | −39.25 | −15.50 |
| Isokotomolide A | −39.10 | −12.50 |
| Akolactone B | −37.95 | −17.75 |
| Obtusilactone | −37.75 | −21.90 |
| Mahubenolide | −36.31 | −12.60 |
| Liseakolide B | −36.25 | −12.10 |
| Litseakolide A | −36.15 | −13.60 |
| Kotomolide A | −34.30 | −13.30 |
| Litsenolide | −33.80 | −16.60 |
| Akolactone A | −30.50 | −15.40 |
| Subamolide A | −28.60 | −18.00 |

## 2. Methods

### 2.1. In silico molecular docking procedure

The tridimensional structure of the human Barrier-to-Autointegration Factor 1 (BAF1) was retrieved from the Protein Data Bank (www.rcsb.org) under the PDB code 1CI4 (Umland et al., 2000). Docking experiments were performed with the GOLD software (GOLD 5.3 release, Cambridge Crystallographic Data Centre, Cambridge, UK). Before starting the docking procedure, the structure of the ligands has been optimized using a classical Monte Carlo conformational searching procedure as described in the BOSS software (Jorgensen et al., 2004). Drug properties were calculated with the BOSS 4.9 software (Jorgensen and Tirado-Rives, 2005) according to published procedures (Vergoten et al., 2003; Lagant et al., 2004).

Based on shape complementarity criteria, the binding site for the Ob-B ligand has been defined around amino acid residue Ile-26 of BAF1. Shape complementarity and geometry considerations are in favor of a docking grid centered in the volume defined by this amino acid. Within the binding site, side chains of specific amino acids have been considered

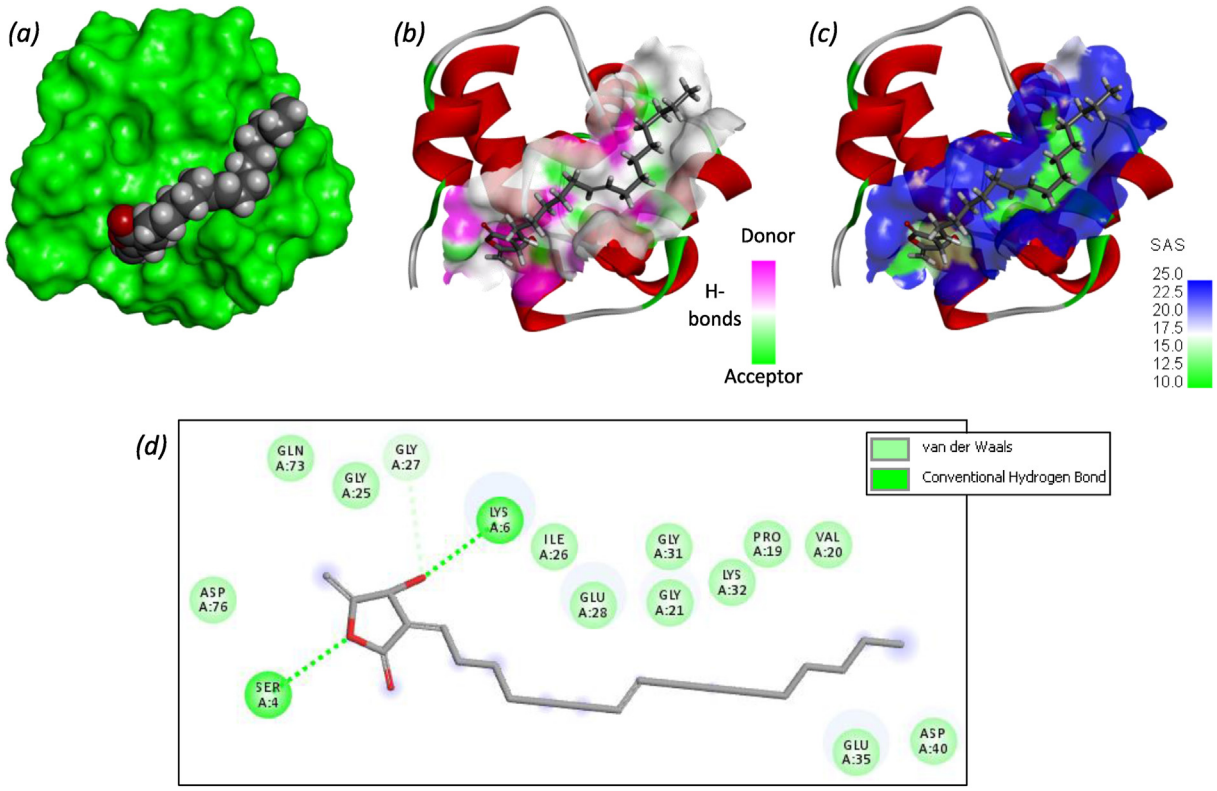


**Fig. 2.** Molecular model of Ob-B bound to BAF1. (*a*) The compound extends along the protein surface and fits into a groove over the entire length of the protein (green). Panels (*b* and *c*) show a detailed view of the compound in the binding site, with (*b*) the H-bond donor/acceptor groups and (*c*) the solvent-accessible surface (SAS) defined. (*d*) Binding map contacts for Ob-B bound to BAF1. (For interpretation of the references to color in this figure legend, the reader is referred to the Web version of this article.)

as fully flexible. The flexible amino acids are ile26, glu28, leu30, lys32, glu35, cys37, val39, leu63, asn70, and gln73. The ligand is always defined as flexible during the docking procedure. Up to 100 poses that are energetically reasonable were kept while searching for the correct binding mode of the ligand. The decision to keep a trial pose is based on ranked poses, using the PLP fitness scoring function (which is the default in GOLD version 5.3 used here (Jones et al., 1997)). The same procedure was used to establish molecular models for all compounds listed in Table 1. The empirical potential energy of interaction ΔE for the ranked complexes is evaluated using the simple expression ΔE(interaction) = E(complex) - (E(protein) + E(ligand)). For that purpose, the Spectroscopic Empirical Potential Energy function SPASIBA and the corresponding parameters were used. Free energies of hydration (ΔG) were estimated using the MM/GBSA model in Monte Carlo simulations within the BOSS software (Jorgensen et al., 2004). The stability of the receptor-ligand complex is evaluated through the empirical potential energy of interaction (Vergoten et al., 2003; Lagant et al., 2004). The Molecular Mechanics/Generalized Born Surface Area (MM/GBSA) procedure was used to evaluate free energies of hydration (within the BOSS program (Jorgensen et al., 2005)), in relation with aqueous solubility (Zafar and Reynisson, 2016). Molecular graphics and analysis were performed using Discovery Studio Visualizer, Biovia 2020 (Dassault Systèmes BIOVIA Discovery Studio Visualizer 2020, San Diego, Dassault Systèmes, 2020).

The two most widely used methods to investigate protein-ligand stability and affinity are Molecular Dynamics (MD) and Monte Carlo (MC) simulations. Both methods use an empirical force field to control the total energy (MC, energy minimization) and forces (MD, Newton equations of motion). To use MD simulations confidently, a force field parameterized for dynamical properties is required. The development of a reliable and accurate force field for the conformational analysis is a concern. It requires accuracy of the force field over the whole potential surface, rather than in the region of the global minimum (Homans, 1990). The most used academic force fields (CHARMM, AMBER, GROMOS) do not exhibit the required vibrational spectroscopic quality. Determination of normal modes on a minimized protein structure using the above force fields can result in imaginary wavenumbers corresponding to maxima in the potential energy (transition states, mainly due to inadequate barriers to internal rotation). The spectroscopic SPASIBA force field has been specifically developed to provide refined empirical molecular mechanics force field parameters, as described in other studies (Vergoten et al., 2003; Meziane-Tani et al., 2006). For this reason, we preferred to use MC simulations rather than MD which requires a substantial increase in computer time to achieve the same level of convergence (Jorgensen and Tirado-Rives, 1996).

## 3. Results

### 3.1. Obtusilactone B structure and properties

The structure of Obtusilactone B (Ob-B) is presented in Fig. 1. This natural product bears a γ-lactone with an exocyclic methylene, and a long endoolefinic alkyl side chain (–$(CH_2)_5$–CH═CH–$(CH_2)_7$–$CH_3$) with a C7′-C8′ double bond (Niwa et al., 1975c). An incorrect structure of Ob-B, without this central double bond, is mentioned in PubChem (CID: 180554; C19H32O3) whereas the correct structure has been cited as isoobtusilactone B (CID: 101286261; $C_{21}H_{34}O_3$). Ob-B is a small molecule (Mw: 334.5 g/mmol, molecular volume: 1334 Å3) with a polar head and a non-polar tail. It is essentially a hydrophobic molecule (calculated logP = 5.3), with a hydrophobic solvent-accessible surface area (SASA) largely superior to the hydrophilic SASA (hydrophobic SASA 618.1 Å2 and hydrophilic SASA 96.6 Å2, calculated with a probe of 1.4 Å radius).

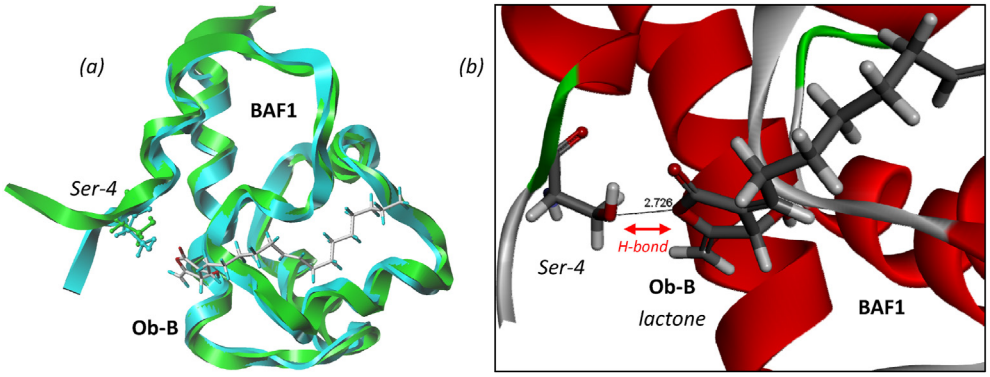


**Fig. 3.** Superimposed models of the crystallographic structure of BAF1 (PDB: 1CI4, in green) and our model of Ob-B bound to BAF1 (in cyan). The Ser-4 residue corresponds to the phosphorylation site of BAF1. This residue lies in a non-structured flexible region of the protein. A conformational analysis (Monte Carlo) of this domain has been performed, leading to the Ob-B-BAF1 complex with an O–O distance of 2.726 Å between the Ser-4 OH residue and the O-lactone of Ob-B. The distance is compatible with the formation of a H-bond interaction. (For interpretation of the references to color in this figure legend, the reader is referred to the Web version of this article.)

### 3.2. Interaction between Ob-B and BAF1

Models of Ob-B bound to BAF1 were constructed starting from the crystal structure of human BAF1 (PDB code 1CI4). It is a small conserved 10-kDa chromatin protein. The structure corresponds to a homodimer within the crystallographic asymmetric unit, each monomer containing a helix-hairpin-helix DNA binding motif (Umland et al., 2000). In our case, models were elaborated with the protein monomer. The protein is relatively globular, not offering a profound groove or a wide cleft for drug binding. However, there is a kind of groove along the protein, spanning from the DNA-binding side to the emerin-interacting side (Fig. 1b). We could easily identify the potential binding location for Ob-B on the BAF1 surface. The natural product is almost fully extended into a little gutter with the carbonyl group of the lactone engaged in a H-bond with Lys-6 residue. Several addition van der Waals contacts and alkyl interactions stabilize the protein-drug complex (Fig. 2). This model is reminiscent to that reported initially (Kim et al., 2013). At this site, the calculated the empirical energy of interaction (ΔE) value reached −38.5 kcal/mol, with an energy of hydration (ΔG) of −20.25 kcal/mol. Unsurprisingly, the binding of Ob-B to BAF1 is essentially driven by the lactone moiety, with the long carbon side chain serving as an additional anchor onto the protein surface. The compound essentially extends on the protein surface, crossing the entire length of the protein. The binding cavity remaining well accessible to the solvent and several H-bond donor and acceptor groups are masked by the ligand (Fig. 2). The BAF1-Ob-B complex is stabilized by two main H-bonds and up to 13 van der Walls contacts and alkyl interactions (Fig. 2d).

We noted immediately that the compound occupies the cavity adjacent to the phosphorylation site of the protein. The invariant Ser-4 residue on BAF1 is a major site of phosphorylation during both interphase

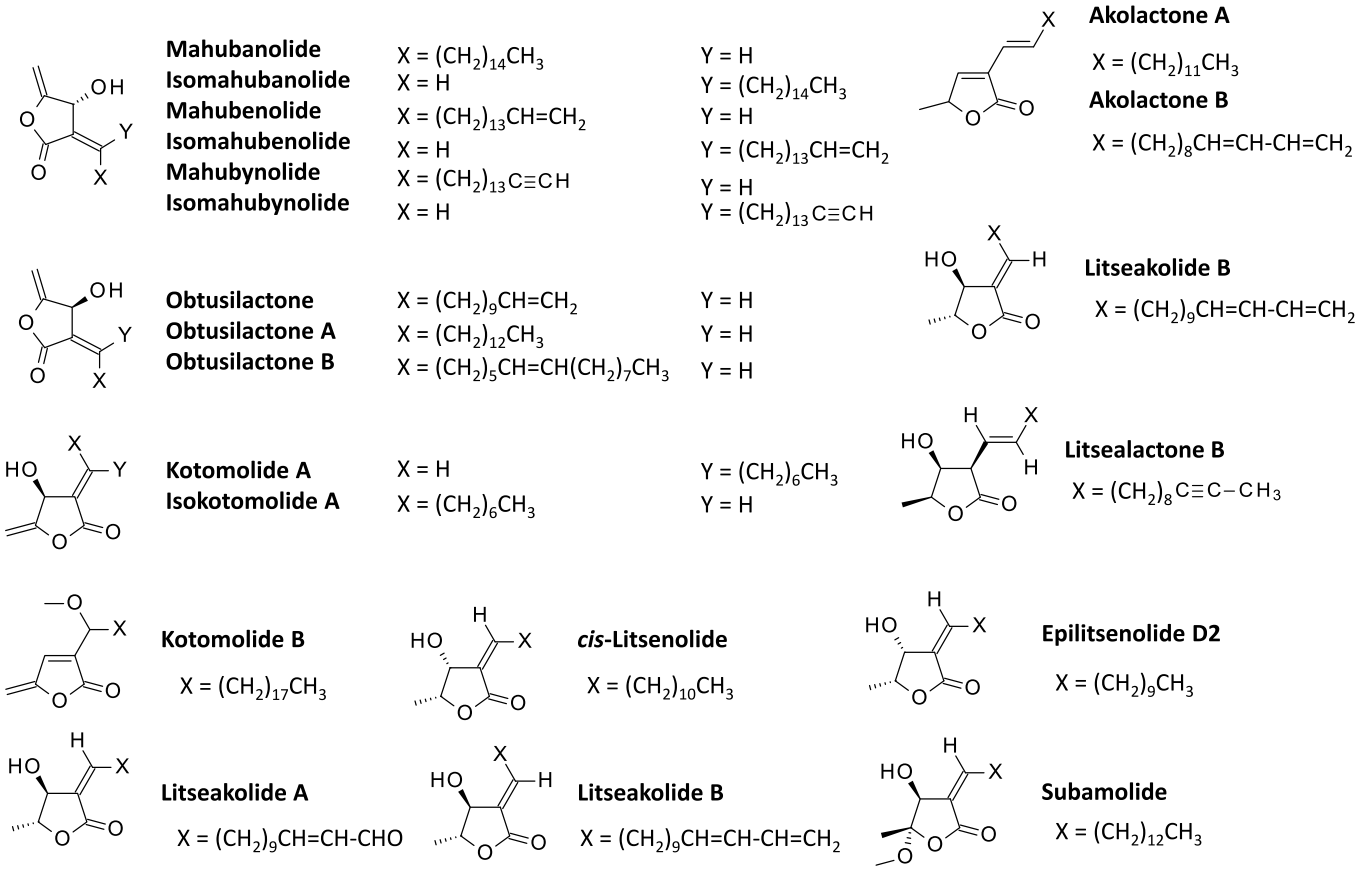


**Fig. 4.** Structures of the tested butanolide derivatives.

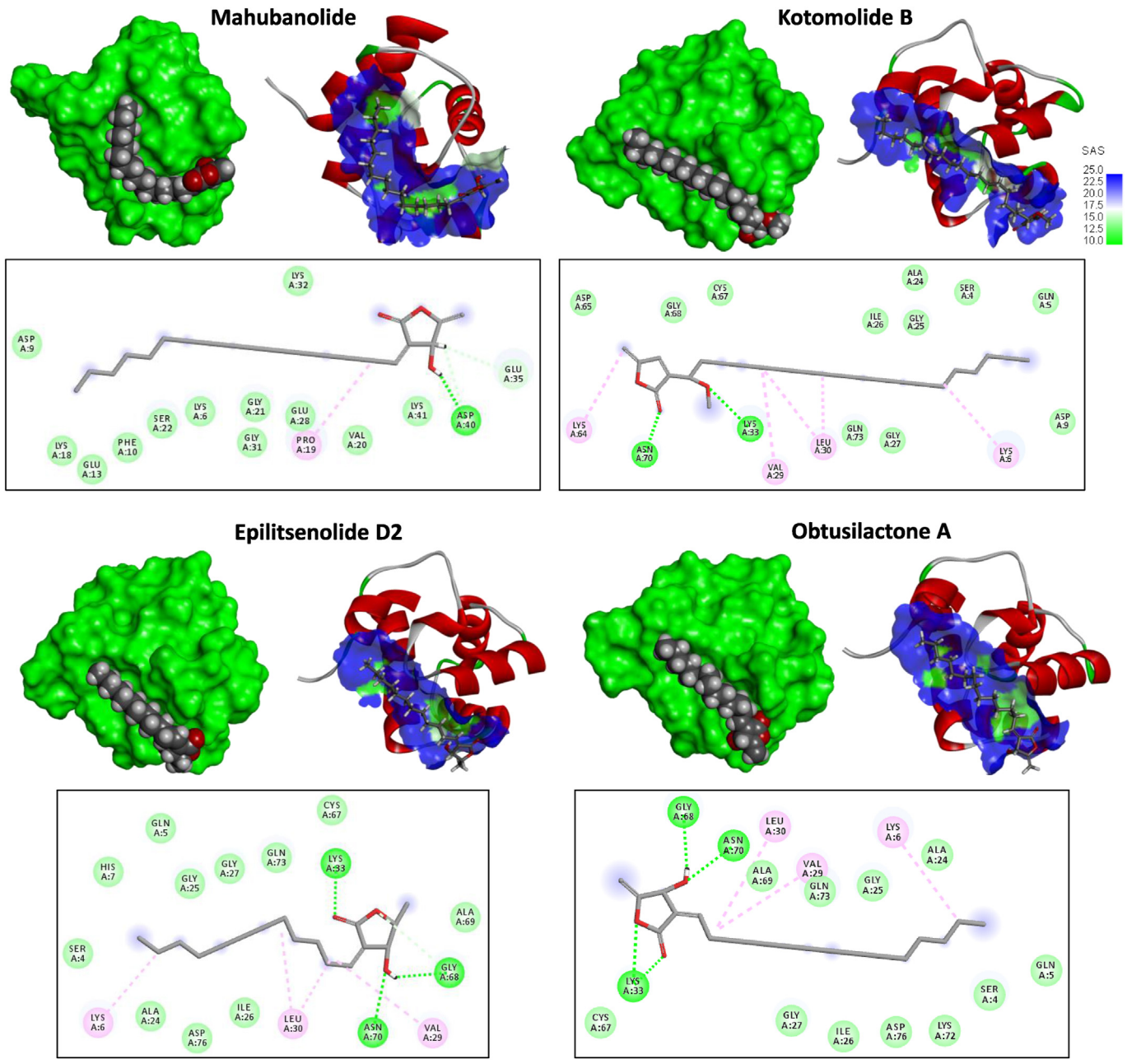


**Fig. 5.** Molecular model of four selected butanolides bound to BAF1. In each case, the compound bound to the BAF1 protein (in green) is presented, together with a close-up view of the compound-binding site (solvent-accessible surface (SAS) with the indicated color code). A binding map for each compound is also included. (For interpretation of the references to color in this figure legend, the reader is referred to the Web version of this article.)

and mitosis (Bengtsson and Wilson, 2006; Zhuang et al., 2014). The BAF1 protein can be successively phosphorylated by VRK1 on Ser-4 and Thr-3 (Marcelot et al., 2021). We noted the establishment of a potential H-bond between Ser-4 and the oxygen lactone of Ob-B, as shown in Fig. 3. The lactone ring of the compound faces the hydroxyl group of Ser-4, within a distance (2.7 Å) fully compatible with a potential H-bond. Therefore, the accessibility to this site is likely reduced upon drug binding, possibly explaining the observed inhibition of VRK1-dependent phosphorylation of BAF1 in the presence of Ob-B (Kim et al., 2013). To sum up this first part, our computational analysis suggests that Ob-B can effectively form stable complexes BAF1, in agreement with the initial experimental data (Kim et al., 2013). A drug binding cavity has been identified and the drug configuration delineated. This model immediately suggested that other butanolide derivatives could interact also with the BAF1 protein.

### 3.3. Binding of other butanolides to BAF1

Natural products bearing a γ-butyrolactone moiety substituted with a long alkyl chain are abundant in nature. γ-Butyrolactones constitute up to about 10% of all known compounds of natural origin (Quintana and Estévez, 2018; Hur et al., 2021). Many of these molecules bear a highly reactive α-methylene-β-lactone, susceptible to form adducts with proteins (Kunzmann et al., 2011). We selected 20 butanolide derivatives with a chemical structure close to that of Ob-B (Fig. 4) and investigated their capacity to form stable complexes with BAF1. For each compound, a docking analysis was performed, and the empirical energies of interaction (ΔE) and free energy of hydration (ΔG) were calculated. The values are collated in Table 1. For four compounds (mahubanolide, litsealactone B, isokotomolide A and akolactone B), two binding poses could be identified, but for clarity only the one with the lowest energy (most

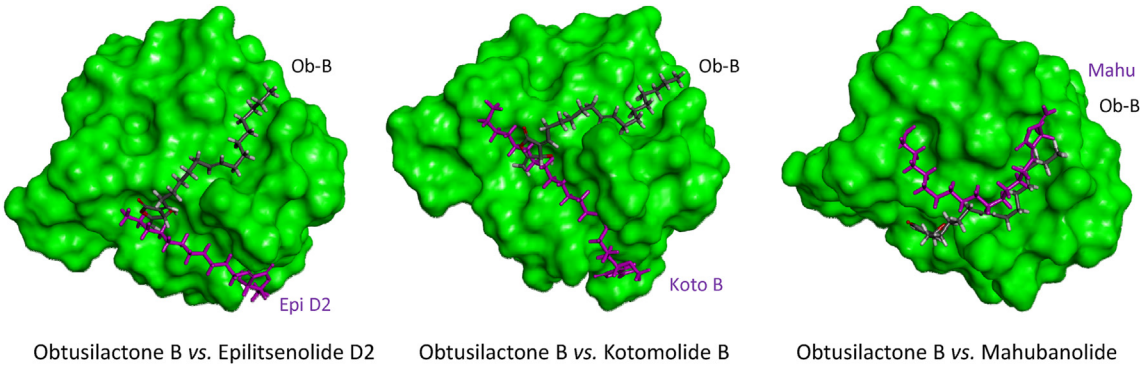


**Fig. 6.** Superimposed models of BAF1 and the indicated butanolide derivatives. Both epilitsenolide D2 and kotomolide B bind preferentially into a groove on the protein surface distinct from that occupied by Ob-B, whereas mahubanolide binds essentially to the same site as Ob-B.

negative ΔE value) is indicated here. We also included in our modeling analysis the other reference compound brazilin which has been reported to bind to BAF1 (Kim et al., 2015). This compound has a totally different structure (tetracyclic homoisoflavonoid) compared to the butanolide derivatives, but it provides a reference point to compare the calculated ΔE-ΔG values (Table 1).

Several butanolide derivatives with a potentially better BAF1-binding capacity than Ob-B have been identified. For half of the compounds, we calculated ΔE values less negative than with Ob-B, suggesting a more favorable interaction with the protein compared to Ob-B. Compounds with a long and flexible alkyl chain provided generally better ΔE values (more negative) than compounds with a shorter side chain. For example, Ob-A with a linear C-13 alkyl chain gave a ΔE of −45.1 kcal/mol, much more favorable than that of Ob-B. The best compound in the series is mahubanolide which possesses a long C-15 alkyl chain. This compound appears to be able to form a very stable complex with BAF1 (Fig. 5). The presence of a terminal double bond (mahubenolide) or triple bond (mahubynolide) is an unfavorable element for BAF1 protein binding.

Another potent compound is kotomolide B with bears a long (C-18) flexible alkyl side chain, forming more stable complexes with BAF1 compared to kotomolide A with a shorter side chain. But this compound fits into a cavity on the BAF1 protein surface distinct from that of Ob-B. The same observation was made with epilitsenolide D2 which also prefers the transversal site, different from that of Ob-B, as illustrated in Fig. 6. The configuration of BAF1-bound mahubanolide is relatively similar to that of Ob-B, whereas both kotomolide B and epilitsenolide D2 preferentially adopt a very distinct orientation (Fig. 6). For this reason, the direct drug-to-drug comparison is a little complicated. However, we could note the potential importance of the exocyclic methylene unit, certainly acting as a positive element for protein binding. In most cases (but not all), the compounds lacking this exocyclic $=CH_2$ provided less stable complexes than those possessing this group. This is the case for the litsenolide series (including litseakolides A-B), subamolide and akolactone A which do not form very stable complexes with BAF1. The 5-exomethylene 4-hydroxy lactone unit common to compounds like Ob-B and mahubanolide is apparently important for the protein interaction. Altogether, the computational analysis indicates that other butanolide derivatives with BAF1-binding capacity superior to our references Ob-B and brazilin can be proposed. The modeling analysis shall be useful to help the identification of new BAF1 binders.

## 4. Conclusion

Butanolide lactones have shown a variety of biological effects including anti-inflammatory, antibacterial, antiprotozoal and anticancer effects. In this class of natural products, the obtusilactone group of compounds has revealed noticeable anticancer effects. The exact mechanism of action of these compounds is not well known. Ob-A has been shown to cause DNA damages and to affect mitochondrial activities in cancer cells (Wang et al., 2010). Its homolog isoobtusilactone A was found to up-regulate the expression of death receptor 5 (DR5) in hepatoma cells (Chen et al., 2012). This compound is also a mitochondrial perturbating agent, promoting the production of reactive oxygen species (ROS) in cancer cells (Kuo et al., 2007; Chen et al., 2007a, 2008, 2008; Liu et al., 2008). The related compound Ob-B has been much less investigated than (iso)Ob-A. Nevertheless, this compound was found to bind to BAF1, causing abnormal nuclear envelope dynamics and inhibition of cancer cell growth, via the suppression of VRK1-mediated phosphorylation of BAF1 (Kim et al., 2013). Ob-B is one of the rare BAF1 inhibitors known thus far. This consideration gave us the impetus to search for other butanolide compounds susceptible to bind to BAF1. A series of 20 compounds was selected and tested for their capacity to form stable complexes with BAF1. Several compounds potentially able to bind more strongly to BAF1 than Ob-B have been identified, including different 2-alkylidene-3-hydroxy-butyrolactones such as mahubanolide, kotomolide B and epilitsenolide D2. These compounds belong to the family of Lauraceae lactones (Rollinson et al., 1981). Their mechanism of action and molecular target(s) are not always well-defined at present. For example, a recent study revealed that isokotomolide A functions as an inducer of autophagy and apoptosis *in vitro* and *in vivo* against melanoma (Li et al., 2020). It also induces apoptosis in human non-small cell lung cancer cells (Chen et al., 2007b). Our analysis suggests that this compound, like Ob-B, could function via an inhibition of BAF1, at least partially. The present study raises novel perspectives for the characterization and design of BAF1-interacting small molecules. The discovery of BAF1 inhibitors is important because the protein plays a role in cancers and other human diseases (Sears and Roux, 2020; Halfmann and Roux, 2021). Notably BAF1 plays roles in various viral diseases. The protein participates to the regulation of gene expression of Ebola virus (Vidal et al., 2021) and acts as a defense against vaccinia virus infection (Jamin et al., 2014). BAF1 functions as inhibitor of retrovirus, poxvirus, and herpesvirus infection (Wiebe and Jamin, 2016). Therefore, small molecule modulators of the protein activity may be useful to combat viral diseases.

## Funding

This research did not receive any specific grant from funding agencies in the public, commercial, or not-for-profit sectors.

## CRediT authorship contribution statement

**Christian Bailly:** Conceptualization, Visualization, Writing – original draft, Writing – review & editing. **Gérard Vergoten:** Investigation, Visualization, Software.

## Declaration of competing interest

The authors declare that they have no known competing financial interests or personal relationships that could have appeared to influence the work reported in this paper.

## References


Bailly, C., 2021. Anticancer butanolides and lignans from the makko tree, *Machilus thunbergii* Sieb. & Zucc. Trends Phytochem. Res. 5, 136–147.

Bengtsson, L., Wilson, K.L., 2006. Barrier-to-autointegration factor phosphorylation on Ser-4 regulates emerin binding to lamin A in vitro and emerin localization in vivo. Mol. Biol. Cell 17, 1154–1163.

Bradley, C.M., Ronning, D.R., Ghirlando, R., Craigie, R., Dyda, F., 2005. Structural basis for DNA bridging by barrier-to-autointegration factor. Nat. Struct. Mol. Biol. 12, 935–936.

Burger, M., Schmitt-Koopmann, C., Leroux, J.C., 2020. DNA unchained: two assays to discover and study inhibitors of the DNA clustering function of barrier-to-autointegration factor. Sci. Rep. 10, 12301.

Burgess, J.T., Cheong, C.M., Suraweera, A., Sobanski, T., Beard, S., Dave, K., Rose, M., Boucher, D., Croft, L.V., Adams, M.N., O'Byrne, K., Richard, D.J., Bolderson, E., 2021. Barrier-to-autointegration-factor (Banf1) modulates DNA double-strand break repair pathway choice via regulation of DNA-dependent kinase (DNA-PK) activity. Nucleic Acids Res. 49, 3294–3307.

Cai, M., Huang, Y., Suh, J.Y., Louis, J.M., Ghirlando, R., Craigie, R., Clore, G.M., 2007. Solution NMR structure of the barrier-to-autointegration factor-Emerin complex. J. Biol. Chem. 282, 14525–14535.

Carrión-Marchante, R., Frezza, V., Salgado-Figueroa, A., Pérez-Morgado, M.I., Martín, M.E., González, V.M., 2021. DNA aptamers against vaccinia-related kinase (VRK) 1 block proliferation in MCF7 breast cancer cells. Pharmaceuticals 14, 473.

Chen, C.Y., Chen, C.H., Lo, Y.C., Wu, B.N., Wang, H.M., Lo, W.L., Yen, C.M., Lin, R.J., 2008. Anticancer activity of isoobtusilactone A from *Cinnamomum kotoense*: involvement of apoptosis, cell-cycle dysregulation, mitochondria regulation, and reactive oxygen species. J. Nat. Prod. 71, 933–940.

Chen, C.Y., Hsu, Y.L., Chen, Y.Y., Hung, J.Y., Huang, M.S., Kuo, P.L., 2007b. Isokotomolide A, a new butanolide extracted from the leaves of Cinnamomum kotoense, arrests cell cycle progression and induces apoptosis through the induction of p53/p21 and the initiation of mitochondrial system in human non-small cell lung cancer A549 cells. Eur. J. Pharmacol. 574, 94–102.

Chen, C.Y., Liu, T.Z., Chen, C.H., Wu, C.C., Cheng, J.T., Yiin, S.J., Shih, M.K., Wu, M.J., Chern, C.L., 2007a. Isoobtusilactone A-induced apoptosis in human hepatoma Hep G2 cells is mediated via increased NADPH oxidase-derived reactive oxygen species (ROS) production and the mitochondria-associated apoptotic mechanisms. Food Chem. Toxicol. 45, 1268–1276.

Chen, C.Y., Yiin, S.J., Hsu, J.L., Wang, W.C., Lin, S.C., Chern, C.L., 2012. Isoobtusilactone A sensitizes human hepatoma Hep G2 cells to TRAIL-induced apoptosis via ROS and CHOP-mediated up-regulation of DR5. J. Agric. Food Chem. 60, 3533–3539.

Couñago, R.M., Allerston, C.K., Savitsky, P., Azevedo, H., Godoi, P.H., Wells, C.I., Mascarello, A., de Souza Gama, F.H., Massirer, K.B., Zuercher, W.J., Guimarães, C.R.W., Gileadi, O., 2017. Structural characterization of human Vaccinia-Related Kinases (VRK) bound to small-molecule inhibitors identifies different P-loop conformations. Sci. Rep. 7, 7501.

Gorjánácz, M., Klerkx, E.P., Galy, V., Santarella, R., López-Iglesias, C., Askjaer, P., Mattaj, I.W., 2007. Caenorhabditis elegans BAF-1 and its kinase VRK-1 participate directly in post-mitotic nuclear envelope assembly. EMBO J. 26, 132–143.

Gorjánácz, M., 2014. Nuclear assembly as a target for anti-cancer therapies. Nucleus 5, 47–55.

Halfmann, C.T., Roux, K.J., 2021. Barrier-to-autointegration factor: a first responder for repair of nuclear ruptures. Cell Cycle 20, 647–660.

Homans, S.W., 1990. A molecular mechanical force field for the conformational analysis of oligosaccharides: comparison of theoretical and crystal structures of Man alpha 1-3Man beta 1-4GlcNAc. Biochemistry 29, 9110–9118.

Hur, J., Jang, J., Sim, J., 2021. A review of the pharmacological activities and recent synthetic advances of gamma-butyrolactones. Int. J. Mol. Sci. 22, 2769.

Jamin, A., Wicklund, A., Wiebe, M.S., 2014. Cell- and virus-mediated regulation of the barrier-to-autointegration factor's phosphorylation state controls its DNA binding, dimerization, subcellular localization, and antipoxviral activity. J. Virol. 88, 5342–5355.

Jones, G., Willett, P., Glen, R.C., Leach, A.R., Taylor, R., 1997. Development and validation of a genetic algorithm for flexible docking. J. Mol. Biol. 267, 727–748.

Jorgensen, W.L., Tirado-Rives, J., 1996. Monte Carlo versus Molecular Dynamics for conformational sampling. J. Phys. Chem. 100, 14508–14513.

Jorgensen, W.L., Tirado-Rives, J., 2005. Molecular modeling of organic and biomolecular systems using BOSS and MCPRO. J. Comput. Chem. 26, 1689–1700.

Jorgensen, W.L., Ulmschneider, J.P., Tirado-Rives, J., 2004. Free energies of hydration from a generalized Born model and an ALL-atom force field. J. Phys. Chem. B 108, 16264–16270.

Kim, S.H., Lyu, H.N., Kim, Y.S., Jeon, Y.H., Kim, W., Kim, S., Lim, J.K., Lee, H.W., Baek, N.I., Choi, K.Y., Lee, J., Kim, K.T., 2015. Brazilin Isolated from Caesalpinia sappan suppresses nuclear envelope reassembly by inhibiting barrier-to-autointegration factor phosphorylation. J. Pharmacol. Exp. Therapeut. 352, 175–184.

Kim, W., Lyu, H.N., Kwon, H.S., Kim, Y.S., Lee, K.H., Kim, D.Y., Chakraborty, G., Choi, K.Y., Yoon, H.S., Kim, K.T., 2013. Obtusilactone B from Machilus Thunbergii targets barrier-to-autointegration factor to treat cancer. Mol. Pharmacol. 83, 367–376.

Kim, Y.S., Kim, S.H., Shin, J., Harikishore, A., Lim, J.K., Jung, Y., Lyu, H.N., Baek, N.I., Choi, K.Y., Yoon, H.S., Kim, K.T., 2014. Luteolin suppresses cancer cell proliferation by targeting vaccinia-related kinase 1. PloS One 9, e109655.

Kunzmann, M.H., Staub, I., Böttcher, T., Sieber, S.A., 2011. Protein reactivity of natural product-derived gamma-butyrolactones. Biochemistry 50, 910–916.

Kuo, P.L., Chen, C.Y., Hsu, Y.L., 2007. Isoobtusilactone A induces cell cycle arrest and apoptosis through reactive oxygen species/apoptosis signal-regulating kinase 1 signaling pathway in human breast cancer cells. Canc. Res. 67, 7406–7420.

Lagant, P., Nolde, D., Stote, R., Vergoten, G., Karplus, M., 2004. Increasing normal modes analysis accuracy: the SPASIBA spectroscopic force field introduced into the CHARMM program. J. Phys. Chem. 108, 4019–4029.

Li, J., Chen, C.Y., Huang, J.Y., Wang, L., Xu, Z., Kang, W., Lin, M.H., Wang, H.D., 2020. Isokotomolide A from *Cinnamomum kotoense* induce melanoma autophagy and apoptosis in vivo and in vitro. Oxid. Med. Cell. Longev. 2020 3425147.

Li, J., Hu, B., Fang, L., Gao, Y., Shi, S., He, H., Liu, X., Yuan, C., 2018. Barrier-to-autointegration factor 1: a novel biomarker for gastric cancer. Oncol. Lett. 16, 6488–6494.

Li, J., Wang, T., Pei, L., Jing, J., Hu, W., Sun, T., Liu, H., 2017. Expression of VRK1 and the downstream gene BANF1 in esophageal cancer. Biomed. Pharmacother. 89, 1086–1091.

Lin, Y.H., Chen, C.Y., Chou, L.Y., Chen, C.H., Kang, L., Wang, C.Z., 2017. Enhancement of bone marrow-derived mesenchymal stem cell osteogenesis and new bone formation in rats by obtusilactone A. Int. J. Mol. Sci. 18, 2422.

Liu, T.Z., Cheng, J.T., Yiin, S.J., Chen, C.Y., Chen, C.H., Wu, M.J., Chern, C.L., 2008. Isoobtusilactone A induces both caspase-dependent and -independent apoptosis in Hep G2 cells. Food Chem. Toxicol. 46, 321–327.

Marcelot, A., Petitalot, A., Ropars, V., Le Du, M.H., Samson, C., Dubois, S., Hoffmann, G., Miron, S., Cuniasse, P., Marquez, J.A., Thai, R., Theillet, F.X., Zinn-Justin, S., 2021. Di-phosphorylated BAF shows altered structural dynamics and binding to DNA, but interacts with its nuclear envelope partners. Nucleic Acids Res. 49, 3841–3855.

Meziane-Tani, M., Lagant, P., Semmoud, A., Vergoten, G., 2006. The SPASIBA force field for chondroitin sulfate: vibrational analysis of D-glucuronic and N-acetyl-D-galactosamine 4-sulfate sodium salts. J. Phys. Chem. 110, 11359–11370.

Nichols, R.J., Wiebe, M.S., Traktman, P., 2006. The vaccinia-related kinases phosphorylate the N' terminus of BAF, regulating its interaction with DNA and its retention in the nucleus. Mol. Biol. Cell 17, 2451–2464.

Niwa, M., Iguchi, M., Yamamura, S., 1977. The isolation and structure of C19-obtusilactone dimer. Chem. Lett. 581–582.

Niwa, M., Iguchi, M., Yamamura, S., 1975b. The isolation and structure of obtusilactone. Tetrahedron Lett. 19, 1539–1542.

Niwa, M., Iguchi, M., Yamamura, S., 1975c. The structures of C17-obtusilactone dimer and two C21-obtusilactones. Tetrahedron Lett. 49, 4395–4398.

Niwa, M., Iguchi, M., Yamamura, S., 1975a. Three new obtusilactones from *Lindera obtusiloba* Blume. Chem. Lett. 655–658.

Quintana, J., Estévez, F., 2018. Recent advances on cytotoxic sesquiterpene lactones. Curr. Pharmaceut. Des. 24, 4355–4361.

Ren, Z., Geng, J., Xiong, C., Li, X., Li, Y., Li, J., Liu, H., 2020. Downregulation of VRK1 reduces the expression of BANF1 and suppresses the proliferative and migratory activity of esophageal cancer cells. Oncol. Lett. 20, 1163–1170.

Rollinson, S.W., Amos, R.A., Katzenellenbogen, J.A., 1981. Total synthesis of Lauraceae lactones: obtusilactones, litsenolides, and mahubanolides. J. Am. Chem. Soc. 103, 4114–4125.

Sears, R.M., Roux, K.J., 2020. Diverse cellular functions of barrier-to-autointegration factor and its roles in disease. J. Cell Sci. 133, 246546.

Serafim, R.A.M., de Souza Gama, F.H., Dutra, L.A., Dos Reis, C.V., Vasconcelos, S.N.S., da Silva Santiago, A., Takarada, J.E., Di Pillo, F., Azevedo, H., Mascarello, A., Elkins, J.M., Massirer, K.B., Gileadi, O., Guimarães, C.R.W., Couñago, R.M., 2019. Development of pyridine-based inhibitors for the human vaccinia-related kinases 1 and 2. ACS Med. Chem. Lett. 10, 1266–1271.

Shen, Q., Eun, J.W., Lee, K., Kim, H.S., Yang, H.D., Kim, S.Y., Lee, E.K., Kim, T., Kang, K., Kim, S., Min, D.H., Oh, S.N., Lee, Y.J., Moon, H., Ro, S.W., Park, W.S., Lee, J.Y., Nam, S.W., 2018. Barrier to autointegration factor 1, procollagen-lysine, 2-oxoglutarate 5-dioxygenase 3, and splicing factor 3b subunit 4 as early-stage cancer decision markers and drivers of hepatocellular carcinoma. Hepatology 67, 1360–1377.

Umland, T.C., Wei, S.Q., Craigie, R., Davies, D.R., 2000. Structural basis of DNA bridging by barrier-to-autointegration factor. Biochemistry 39, 9130–9138.

Vergoten, G., Mazur, I., Lagant, P., Michalski, J.C., Zanetta, J.P., 2003. The SPASIBA force field as an essential tool for studying the structure and dynamics of saccharides. Biochimie 85, 65–73.

Vidal, S., Sánchez-Aparicio, M., Seoane, R., El Motiam, A., Nelson, E.V., Bouzaher, Y.H., Baz-Martínez, M., García-Dorival, I., Gonzalo, S., Vázquez, E., Vidal, A., Muñoz-Fontela, C., García-Sastre, A., Rivas, C., 2021. Expression of the Ebola virus VP24 protein compromises the integrity of the nuclear envelope and induces a laminopathy-like cellular phenotype. mBio 12, e0097221.

Wang, H.M., Cheng, K.C., Lin, C.J., Hsu, S.W., Fang, W.C., Hsu, T.F., Chiu, C.C., Chang, H.W., Hsu, C.H., Lee, A.Y., 2010. Obtusilactone A and (-)-sesamin induce

apoptosis in human lung cancer cells by inhibiting mitochondrial Lon protease and activating DNA damage checkpoints. Canc. Sci. 101, 2612–2620.
Wiebe, M.S., Jamin, A., 2016. The barrier to autointegration factor: interlocking antiviral defense with genome maintenance. J. Virol. 90, 3806–3809.
Zafar, A., Reynisson, J., 2016. Hydration free energy as a molecular descriptor in drug design: a feasibility study. Mol. Inform. 35, 207–214.
Zhang, G., 2020. Expression and prognostic significance of BANF1 in triple-negative breast cancer. Canc. Manag. Res. 12, 145–150.
Zhuang, X., Semenova, E., Maric, D., Craigie, R., 2014. Dephosphorylation of barrier-to-autointegration factor by protein phosphatase 4 and its role in cell mitosis. J. Biol. Chem. 289, 1119–1127.